HETEROGENEOUS POISONING OF THE CRITICAL HTGR TEST FACILITY KAHTER: A STUDY FOR THE INITIAL LOADING OF PEBBLE BED POWER REACTORS

FISSION REACTORS

VOLKER DRÜKE, DETLEF FILGES, RAHIM NABBI,
RALF D. NEEF, NORBERT PAUL, and HARTWIG SCHAAL
Institut für Reaktorentwicklung der Kernforschungsanlage Jülich GmbH
Postfach 1913, D-5170 Jülich, Germany

Received October 23, 1980
Accepted for Publication April 10, 1981

Investigation of the initial core poisoning of the pebble bed high temperature reactor has been made by experiments and by checking computations. In following the example of the thorium high-temperature reactor THTR-300, THTR absorber elements poisoned with hafnium-boron were added to the THTR fuel and graphite elements of the KAHTER core. Three different hafnium-boron poisoned core loadings, corresponding to 2.7, 5.3, and 8% reactivity compensation, were used in the experiments. For purposes of comparison, two cores poisoned exclusively with boron were also studied. The poisoning of these cores corresponds to 2.7 and 8% reactivity compensation, respectively.

The experiments and checking computations should serve to test the accuracy of the theoretical models and data sets in modeling the reactivity effects of absorber poisoned elements in the THTR. In particular, the applicability of the nuclear data of hafnium and the treatment of resonance calculations should be verified.

In addition to determining critical masses and k_{eff}, special emphasis was placed in the experiments on the exact determination of all reactivity effects. In some cases, repeated loading of a configuration also provided a measure of the reproducibility of k_{eff}. The experiments were checked computationally using the GAMTEREX code package and the program system RSYST. These two computation packages contain different data bases, although the hafnium data are identical, and the computing models differ in certain phases of the calculations. Both code systems compute k_{eff} values to within the present accuracy requirements, whereas the program system RSYST gives better agreement with experimental measurements.

I. INTRODUCTION AND MOTIVATION

In large pebble bed high temperature gas-cooled reactors (HTGRs), e.g., the thorium high temperature reactor THTR-300 MW(electric), the excess reactivity of the initial core is compensated for by statistically distributed spherical elements containing boron and hafnium. The aim of this work was to test the theoretical models, codes, and data bases used for nuclear layout and safety analysis due to poisoned pebble bed cores. For this purpose several experiments with different mixtures of fuel, moderator, and absorber elements were performed at the critical facility Kritische Anlage Hochtemperatur-Reaktor (KAHTER). The comparison of the experimental results with theoretical calculations particularly had to yield a suitable calculational model of the random distribution of the pebbles and to prove the validity of the nuclear data of hafnium.

II. DESCRIPTION OF EXPERIMENTS

II.A. The KAHTER Facility

In the frame of the development of the high temperature gas-cooled pebble-bed reactor, the critical facility KAHTER was constructed and built up in 1973 (Ref. 1).

Figure 1 shows a schematic view. The core has a diameter of 216 cm and a maximum height of 240 cm; it is reflected on the bottom by 60-cm-thick graphite, which decreases to 44 cm at the center. Circumferentially, a graphite reflector exists with a thickness of 40 cm, and a top reflector with a height of 10 up to 50 cm may be installed. This core can be filled with up to 49 000 elements of the pebble type (6 cm in diameter).

To control or shut down this system, the KAHTER facility has eight control rods containing

1981

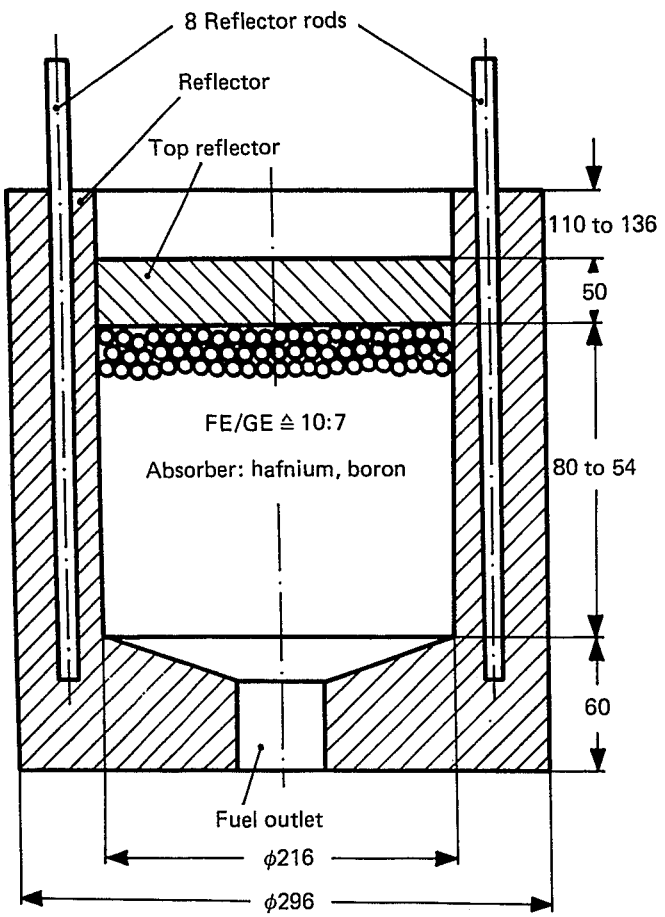

Fig. 1. Sectional view of KAHTER (dimensions in centimetres).

B_4C. To measure reaction rates small (6-cm-diam) tubes of aluminum are positioned in the core in radial and axial directions. For the same purpose, bore holes exist in the reflectors.

II.B. Types of Spherical Elements

The core is composed of

1. fuel elements (FEs)
2. graphite elements (GEs)
3. absorber elements (AEs).

As fuel elements, THTR (Ref. 2) and Arbeitsgemeinschaft Versuchs Reaktor (AVR) (Ref. 3) elements were used. The most important nuclides of spherical elements are listed in Table I. The boron AEs contain a pellet with homogeneous mixture of graphite and boron nitride (Fig. 2).

II.C. Core Configurations

To investigate cores with poisoned elements, six different core configurations were performed. In detail these were one unpoisoned core as reference

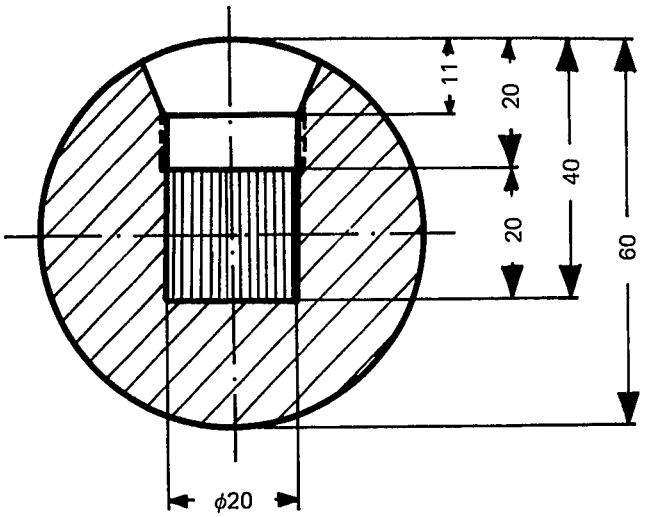

Fig. 2. Sectional view of boron absorber element (dimensions in millimetres).

and two boron poisoned and three hafnium poisoned cores. Table II shows the experimental data.

Normally THTR elements were used as fuel elements. But since few THTR elements were available, AVR fuel elements were added to reach the critical mass for the two cores B2 and H3. The pebble-bed height is measured from the bottom of the reflector up to the surface of the pebble bed. The ratio of fuel elements to graphite and absorber elements is roughly 10:7. The symmetry and the homogeneity of the core loading were tested by measuring the reactivity worth of each absorber rod. To check reproducibility the core B2 was built up three times and the reference core twice (see Sec. III).

III. EXPERIMENTAL RESULTS–CRITICAL MASSES AND k_{eff} VALUES

The k_{eff} values were determined by measuring the excess reactivity with the inhour method. The given k_{eff} values are related to a core assembly with bore holes in the top reflector and with ionization chambers in the bottom reflector (see Figs. 3 and 4). In case of subcriticality the k_{eff} value was determined by the pulsed neutron method.[4]

Table III shows the amount of ^{235}U and the k_{eff} values of different core configurations. In the calculations it was impossible to take into account the presence of ionization chambers in the bottom reflector and the fact that neutrons are scattered back from the surrounding concrete walls into the assembly. Therefore, additional measurements were performed where the ionization chambers were removed from the bottom reflector or where the assembly was covered with cadmium. These measurements were done for a few selected core configurations only. The values for the other core

TABLE I

Nuclide Concentrations of Used Spherical Elements (g)

Nuclide	Fuel Elements		Absorber Elements		Graphite Elements
	AVR	THTR	Boron	Hafnium	
^{234}U	0.00550	0.01030			
^{235}U	1.00059	0.96187			
^{236}U	0.00312				
^{238}U	0.06579	0.06190			
^{232}Th	5.03600	10.2			
Carbon	192.70	192.0	182.27	192.0	190.80
B_{nat}			0.2910	0.040	
Hf_{nat}				4.20	

TABLE II

KAHTER Core Configurations

Core Configuration	Number of Elements				Loading Ratio FE:GE:AE	Pebble Bed Height (cm)
	Fuel		Moderator	Absorber		
	THTR	AVR				
Reference	11 500	0	8 050	0	10: 7:0	151.88 ± 0.5
B1 boron	15 660	0	10 440	435	36:24:1	185.5
B2 boron	17 190	1910	12 415	955	20:13:1	214.0 ± 0.5
H1 hafnium	14 985	0	10 125	405	37:25:1	179.4
H2 hafnium	16 578	0	11 052	614	27:19:1	193.0
H3 hafnium	17 190	1350	12 051	927	20:13:1	208.0

configurations were extrapolated. The influence to the k_{eff} value is shown in the third and fourth columns of Table III. The extrapolated values are given in parentheses. This procedure yielded adjusted k_{eff} values, which can be compared with calculated ones.

IV. THEORETICAL MODELS AND NUCLEAR DATA

To analyze the critical experiments with boron and hafnium absorber elements, we have mainly used codes that are standard codes for HTGR layout calculations at Kernforschungsanlage (KFA)-Jülich. Only some peculiarities, e.g., evaluation of hafnium libraries, required further codes. As standard codes the GAMTEREX (Ref. 5) cycle and the program system RSYST (Ref. 6) have been used. The principle procedure to solve all relevant problems is described in detail in Ref. 7. In this paper, only the special features of the critical facility KAHTER and in particular the model description of the absorber elements are treated.

IV.A. Nuclear Data Libraries for GAMTEREX

IV.A.1. Standard Libraries for HTGR Calculations

The 30-group THERMOS library contains all necessary cross sections in the energy range from $3.9 \cdot 10^{-3}$ to 2.05 eV for moderator, fission, breeding, and $1/v$ absorber materials.

The GAM-I library consists of 68 groups in the energy range from 0.41 eV to 10.0 MeV and contains elastic scattering moments from P_0 to P_3, inelastic and $(n,2n)$ scattering matrices, ν, σ_f, and σ_{tot}. For the elements ^{232}Th and ^{238}U, resonance parameters and σ_{smooth} are available. The quantity σ_{smooth} is the difference between the measured σ_a and that calculated by use of the one-level Breit-Wigner formula. The THERMOS and GAM cross-section library data are

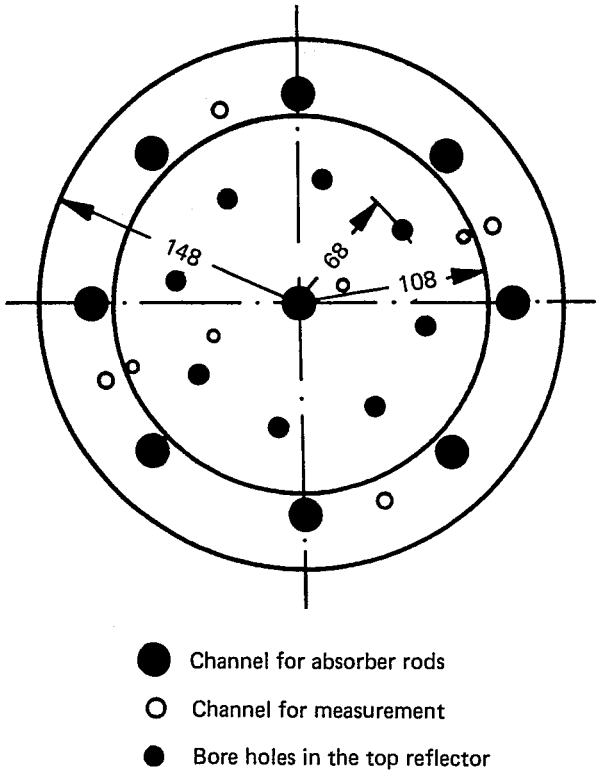

Fig. 3. Top reflector with bore holes and channels (dimensions in centimetres).

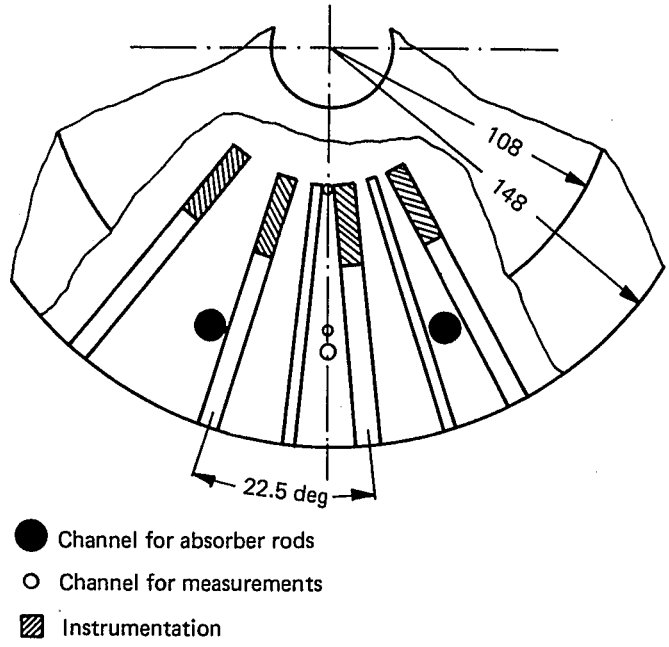

Fig. 4. Sectional view of instrumentation position in bottom reflector (dimensions in centimetres).

either evaluated from ENDF/B-II or especially developed in KFA-Jülich for application to HTGRs.

IV.A.2. Hafnium Data

Only hafnium isotope cross sections did not exist on both THERMOS and GAM libraries. Hence, it was necessary to produce group cross sections of the hafnium isotopes. The problem independent data were taken from the hafnium data collection of Krebs et al.[8] These data are available on tape in ENDF/B-IV format. By use of the SUPERTOG code,[9] it was possible to generate multigroup cross sections. The necessary calculational models and program procedures for the evaluation of hafnium cross sections are described in Sec. IV.C (resonance treatment) and are shown in Fig. 5.

TABLE III

Critical Masses and Experimental k_{eff} Values

Core	Critical Mass ^{235}U (kg)	k_{eff}[a] Measured	Δk Ionization Chambers (%)	Δk Cadmium-Shielding (%)	Δk Total (%)	k_{eff} Corrected
Reference 1	11.0607	0.99562	0.334	(0.215)	0.119	0.99681
Reference 2	11.0607	0.99756	0.358	0.215	0.143	0.99899
B1	15.0618	1.00322	(0.252)	(0.185)	0.067	1.00389
B2a	18.4433	1.00048	(0.187)	(0.160)	0.027	1.00075
B2b	18.4433	0.99660	0.204	(0.160)	0.044	0.99704
B2c	18.4433	0.99939	0.170	(0.160)	0.010	0.99949
H1	14.4126	1.00473	(0.252)	(0.185)	0.067	1.00540
H2	15.9447	1.00428	(0.220)	(0.175)	0.045	1.00473
H3	17.8833	1.00101	(0.170)	(0.160)	0.010	1.00111

[a]With ionization chambers and without cadmium shielding.

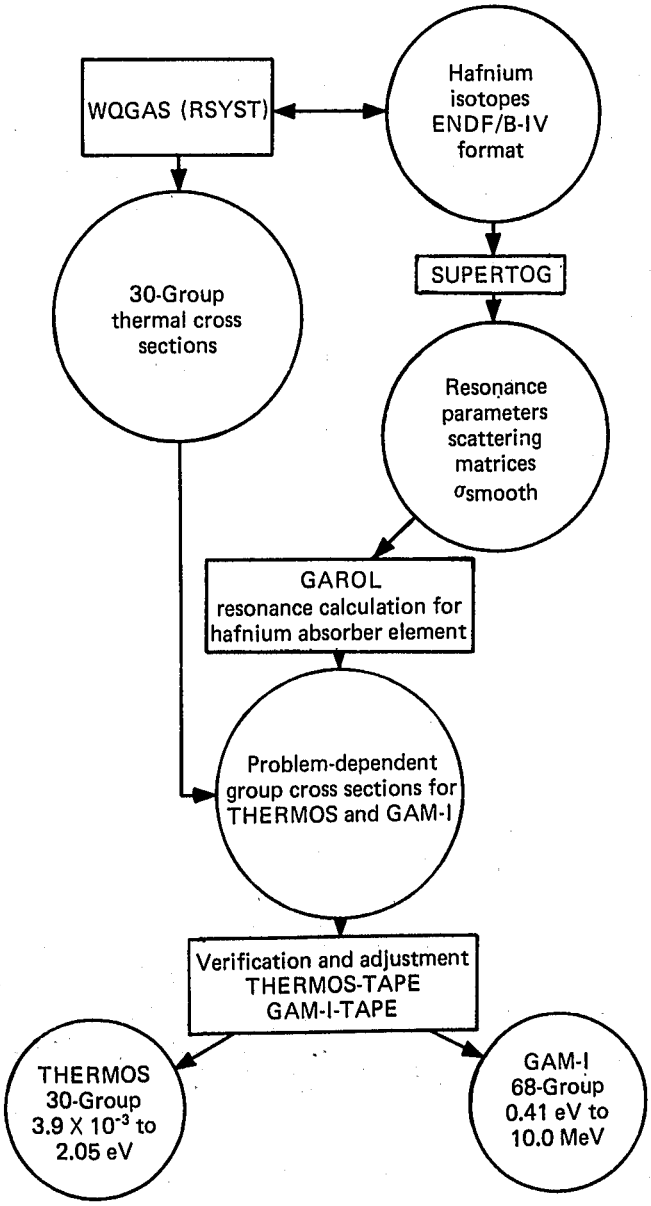

Fig. 5. Flow diagram showing the generation of problem dependent hafnium data for the THERMOS and GAM libraries.

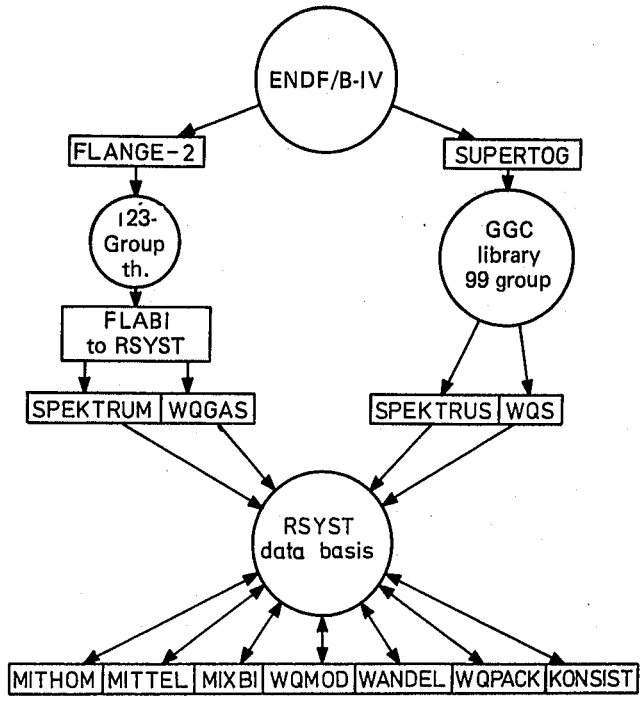

Fig. 6. View of programs used for generating the group constants in RSYST.

IV.B. Nuclear Data Libraries for RSYST

IV.B.1. Standard Libraries

For generation of group constants in the thermal, epithermal, and fast energy range in RSYST, several codes are available. Figure 6 gives an overview of the programs used. For the production of problem dependent group constants, the two problem independent data libraries THERM-123 (thermal data) and GGC (epithermal and fast data) were used. All data are based on ENDF/B-IV.

The THERM-123 library contains moderator and all relevant absorber data (fission materials, fuel materials, etc.) in 123 energy groups of the energy range from 10^{-5} to 1.85 eV.

The GGC library has 99 groups in the energy range from 0.41 eV to 14.9 MeV. The library contains resonance parameters, elastic scattering moments up to P_3, inelastic and $(n,2n)$ scattering matrices, ν, σ_f, σ_{tot}, σ_s, and σ_{smooth}.

Core calculations are based on problem-dependent 53-group cross sections, which are generated from the THERM-123 and GGC libraries, taking into account the downscattering into the thermal energy range. The data of the THERM-123 library are collapsed from 123 to 30 groups and those of the GGC library from 99 to 23 groups. The required spectra are produced by zero-dimensional spectrum calculations in B_N theory. For the thermal energy range, the module SPEKTRUM is used; for the epithermal and fast energy ranges we use the module SPEKTRUS, which performs the resonance calculations in the same manner as the ZUT-DGL program.[10] The procedure to generate the 53-group library is the starting point of all following calculations.

IV.B.2. Hafnium Data

For the hafnium isotopes a special procedure was performed. As in the case of the GAMTEREX calculations, the data of Krebs et al.[8] were used. These data are in the ENDF/B-IV format. Therefore they can be used by the module ENDRES and by the code

SUPERTOG to generate 99-group cross sections for the GGC library.

IV.C. Resonance Calculations

IV.C.1. Fuel Elements in GAM-THERMOS

In the epithermal energy region, resonance parameters of ^{232}Th and ^{238}U are used to calculate the resonance integrals. Because of the double heterogeneous geometry of the fuel elements, these calculations are performed by the ZUT-DGL code.[10] The resulting resonance absorption cross sections are transferred to the GAM-I spectral code, which adds them to σ_{smooth}. Infinitely diluted ^{235}U cross sections already exist on the GAM-I library.

IV.C.2. Hafnium Absorber Elements in GAM-THERMOS

Hafnium is a mixture of different isotopes (see Table IV). Therefore, the resonance calculation was performed by the GAROL code,[11] which allows calculation of up to ten isotopes in correlation to each other. This procedure takes into account the resonance overlapping effect.

To study the influence of grain structure of the HfC particles inside the pellet of the hafnium absorber element, two resonance calculations were performed, one in spherical, the other in double heterogeneous geometry with a grain diameter of 42 μm. The comparison of the results (see Table V) shows that for the natural mixture of hafnium the resonance integrals differ by ~2%, which is inside the error margins of resonance integral calculations. The maximum influence of hafnium to k_{eff} is 8% in the KAHTER cores. Therefore, a difference of 2% in the hafnium resonance integral will change k_{eff} only by a 0.16% maximum. Therefore, it can be stated that a double heterogeneous calculation is not necessary for the epithermal energy region (>0.41 eV). The treatment of the ENDF/B-IV formated hafnium data by SUPERTOG ("smooth" cross sections, scattering matrices, and resonance parameters) and by GAROL (resonance calculations) yields the problem-dependent hafnium cross sections for the GAM-I library (see Fig. 5).

In the thermal energy range from $3.9 \cdot 10^{-3}$ to 2.05 eV, the hafnium group cross sections were also generated by GAROL. A comparison of the hafnium group cross sections in the GAM-I and THERMOS libraries showed differences in the overlapping energy range from 0.41 to 2.05 eV. Hence, it was necessary to perform a $1/v$ correction in the thermal energy range to adjust the THERMOS library. The scattering matrices of the hafnium isotopes were calculated by the code system RSYST using the free gas model. The data for calculation of cross sections using the gas model are given in Table VI.

IV.C.3. Fuel Elements in RSYST

In RSYST, the resonance calculation of the nuclides ^{232}Th, ^{235}U, and ^{238}U is performed considering the double heterogeneous geometry of the fuel elements. The necessary escape probabilities are calculated by the module TERESKU and provided to the module SPEKTRUS, which calculates resonance integrals and spectra, using 99-group cross sections and resonance parameters.

TABLE V

Hafnium Resonance Integrals of the Hafnium Absorber Element

Isotope	Resonance Integral	
	Spherical	Double Heterogeneous (42 μm)
^{176}Hf	191.0	183.0
^{177}Hf	1332.0	1333.0
^{178}Hf	451.7	422.3
^{179}Hf	283.7	282.0
^{180}Hf	23.2	22.7
Natural hafnium	426.1	417.6

TABLE IV

Isotope Composition of Natural Hafnium

Isotope	Frequency (%)
^{174}Hf	0.18
^{176}Hf	5.20
^{177}Hf	18.50
^{178}Hf	27.14
^{179}Hf	13.75
^{180}Hf	35.24

TABLE VI

Data for Generation of Cross-Section Matrices of Hafnium

Isotope	σ_a (b) at 0.0253 eV	Free Scattering Cross Section, σ_s (b)
^{174}Hf	390 ± 55	---
^{176}Hf	28 ± 12	6.33
^{177}Hf	363 ± 23	9.0
^{178}Hf	82 ± 6	9.6
^{179}Hf	44 ± 6	6.85
^{180}Hf	19 ± 4	6.21

IV.C.4. Hafnium Absorber Elements in RSYST

In the 53-energy-group library of RSYST, no cross sections were available for hafnium. Therefore, they had to be generated from the ENDF/B-IV formated data and from the data of the GAM-II library.

In the energy region from 0.414 eV to 14.918 MeV, the 99-group cross sections of hafnium were generated by the module SPEKTRUS (see Fig. 7), using data of the GAM-II library. The resonance calculation by SPEKTRUS treats each hafnium isotope separately. To take into account the mutual influence of the isotopes, an additional resonance calculation was performed with the module RESPU, which uses the GAROL formalism. This procedure leads to cross sections in the energy region from 1.85 eV to 1.234 keV. In detail, the resonance calculation is done as follows: Starting points are hafnium data in the ENDF/B-IV format, and are read by the module ENDRES. This module generates fine-group cross sections by application of the multilevel Breit-Wigner formula. So interference and overlapping of narrow resonances are taken into account. The fine-group boundaries are chosen so that the energy region from 1.85 eV to 1.234 keV is divided into 3000 equidistant lethargy intervals. With the module RESPU the neutron transport equation is solved for the absorber region of the hafnium sphere. Outside this region an infinite moderator is assumed. The RESPU code yields the fine group flux of the absorber region to condense the fine group cross sections (see Fig. 8). These condensed cross sections replace the original cross sections in the 99-group library from group 68 to 93.

In the thermal energy region, the 123-group cross sections of hafnium in the structure of THERM-123 were produced in the same manner as the resonance cross sections, but they were condensed to 123 energy groups (see Fig. 8) in the energy range from 10^{-5} to 1.85 eV.

The 99- and the 123-group cross sections were combined to 53-energy-group cross sections of hafnium following the procedure described in Sec. IV.B.1.

IV.D. Computational Model of Unit Cells in GAM-THERMOS

The unit cell needed for the one-dimensional spectral code THERMOS-Jül is represented in spherical

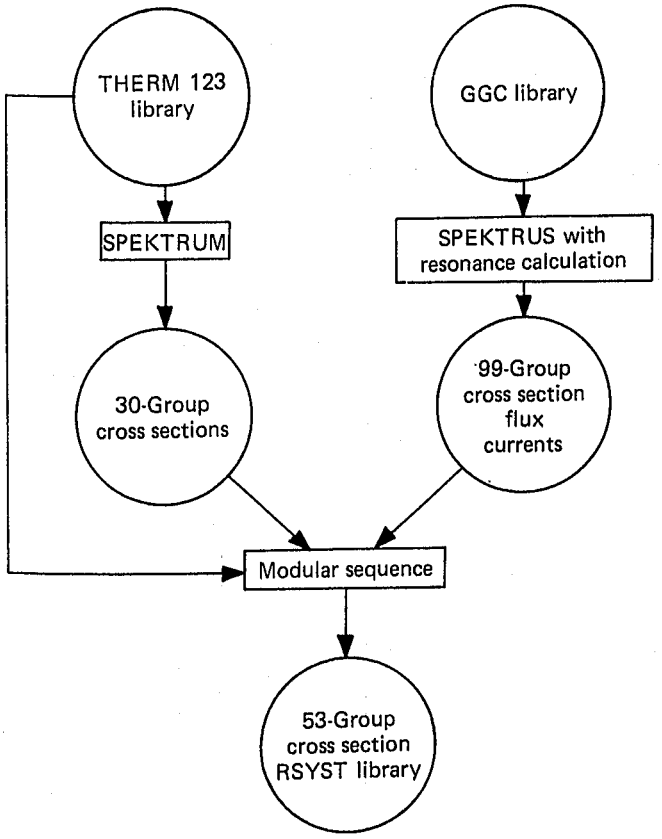

Fig. 7. Modular sequence for generating the problem-dependent group constants.

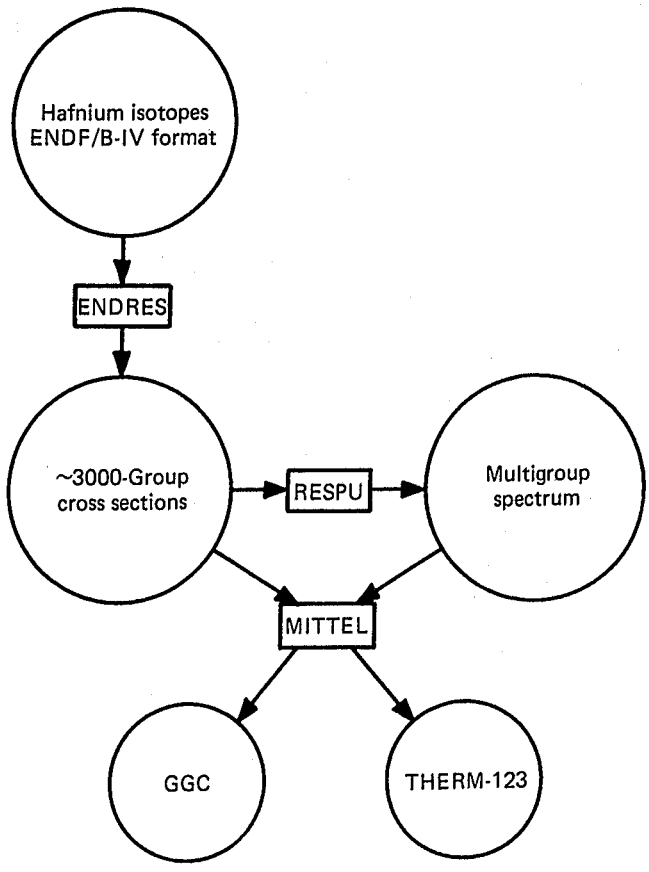

Fig. 8. Flow diagram for calculating the resonance absorption of hafnium.

geometry. In the case of the reference core, the following model was used (see Fig. 9).

In the fuel zone of the spherical fuel element, the coated particles and the matrix graphite were homogenized, taking into account the flux depression inside the coated particles by disadvantage factors calculated by THERMOS-Jül (see Table VII). The second zone is the graphite shell of the THTR fuel element. The third zone contains the air, which surrounds the sphere. Zone 4 of the unit cell is a mixture of 0.7 moderator elements and their surrounding air. Table VIII contains the nuclide concentrations for this model. The effective absorption cross section of graphite in the THTR fuel elements is estimated as 3.8 mb. This value was determined by measuring the concentrations of absorbing elements in the ash content of fuel graphite. The cross section in the THERMOS library is 3.88 mb. Corresponding to this difference of −0.08 mb, a correction was performed by adding a negative boron concentration.

In the case of cores that contain absorber elements, the unit cell is built up in the following manner (see Fig. 10). The center of the unit cell is the absorber element sphere, which is the sphere with the largest flux gradient and therefore must be described exactly. The disadvantage factors of the fuel element were known from earlier calculations. The unit cell consists of four zones. The first is the homogenized absorber matrix, which, in the case of the boron element, is a sphere with the same volume as the real boron nitride cylinder. The second zone is the graphite shell of the absorber element. Zone 3 is the surrounding air. Zone 4 is a mixture of moderator elements, fuel elements, and surrounding air. The nuclide concentrations for all zones of the unit cells are given in Tables IX through XV. These tables contain the homogenized nuclide concentrations, which are used in the GAM-I and EXTERMINATOR-II codes and in the reactor code system RSYST.

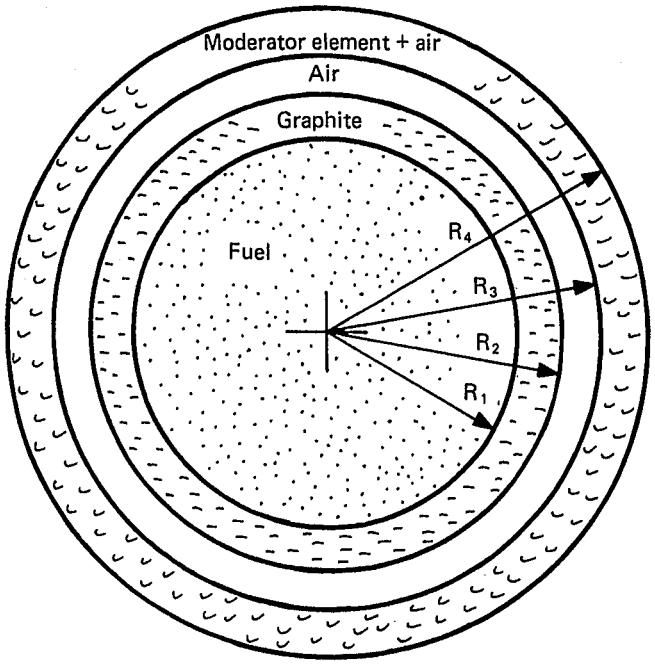

Fig. 9. Cell model for the spectrum calculation in the KAHTER core without absorber elements.

IV.E. Treatment of Boron Elements with GAMTEREX

The spherical boron elements consist of graphite with a cylindrical boron pellet in the center. This pellet has a diameter and a height of 2 cm. For the calculation with THERMOS, the pellet has to be described as a sphere in such a way that its reaction rate should be the same as that of the cylinder. On

TABLE VII

Disadvantage Factors of Coated Particles of THTR Fuel Elements

Upper Energy (eV)	Disadvantage Factors
1.100-02[a]	0.9641
1.988-02	0.9758
3.184-02	0.9818
4.904-02	0.9860
7.046-02	0.9890
9.033-02	0.9908
1.103-01	0.9920
1.352-01	0.9928
1.807-01	0.9938
2.230-01	0.9943
2.757-01	0.9939
3.255-01	0.9940
3.829-01	0.9951
4.809-01	0.9968
6.150-01	0.9978
7.472-01	0.9981
8.528-01	0.9983
9.356-01	0.9982
1.014	0.9982
1.048	0.9976
1.091	0.9973
1.130	0.9969
1.173	0.9966
1.238	0.9979
1.361	0.9990
1.516	0.9995
1.686	0.9993
1.856	0.9995

[a]Read as 1.100×10^{-2}.

TABLE VIII

Nuclide Concentrations of Spherical Unit Cell for KAHTER-Reference Core

Nuclide	THERMOS/ISOSTO				GAM-I DIFF-2D	EXTERMINATOR-II
	Zone 1	Zone 2	Zone 3	Zone 4		
Hydrogen	9.75413-06	1.01764-05	---	6.09889-06	6.12143-06	6.12143-06
Boron	-8.76424-09	-9.14370-09	---	6.71292-08	5.46487-08	2.43976-08
Carbon	8.31506-02	8.67508-02	---	5.19910-02	5.21831-02	5.21831-02
^{232}Th	5.19495-04	---	---	---	8.46303-05	8.46303-05
^{234}U	5.20190-07	---	---	---	8.47435-08	8.47435-08
^{235}U	4.83714-05	---	---	---	7.88014-06	7.88014-06
^{238}U	3.07365-06	---	---	---	5.00724-07	5.00724-07
Nitrogen	1.09403-05	9.71637-06	3.92099-05	2.15340-05	2.14686-05	2.14686-05
Oxygen	1.14292-03	---	1.05199-05	4.05468-06	1.90246-04	1.90246-04
Aluminum	---	---	3.63535-05	---	8.24212-06	8.24212-06

TABLE IX

Nuclide Concentrations of Spherical Unit Cell of KAHTER Core B1

Nuclide	THERMOS/ISOSTO				GAM-I DIFF-2D	EXTERMINATOR-II
	Zone 1	Zone 2	Zone 3	Zone 4		
Hydrogen	2.64713-06	9.88231-06	---	6.18968-06	6.18477-06	6.18477-06
Boron	2.58213-03	7.99145-08	---	2.04584-08	1.51267-06	1.48210-06
Carbon	2.25659-02	8.42433-02	---	5.27649-02	5.27231-02	5.27231-02
^{232}Th	---	---	---	8.72786-05	8.58478-05	8.58478-05
^{234}U	---	---	---	8.73952-08	8.59625-08	8.59625-08
^{235}U	---	---	---	8.12672-06	7.99349-06	7.99349-06
^{238}U	---	---	---	5.16393-07	5.07927-07	5.07927-07
Nitrogen	2.61365-03	1.05688-05	3.92099-05	2.12709-05	2.27463-05	2.27463-05
Oxygen	---	---	1.05199-05	1.96001-04	1.92853-04	1.92853-04
Aluminum	---	---	3.74164-05	---	2.32241-07	2.32241-07

TABLE X

Nuclide Concentrations of Spherical Unit Cell with THTR Fuel Elements of KAHTER Core B2

Nuclide	THERMOS/ISOSTO				GAM-I DIFF-2D	EXTERMINATOR-II
	Zone 1	Zone 2	Zone 3	Zone 4		
Hydrogen	2.64703-06	9.88233-06	---	6.22773-06	6.21888-06	6.21888-06
Boron	2.58204-03	7.99147-08	---	2.35012-08	2.69254-06	2.66181-06
Carbon	2.25650-02	8.42435-02	---	5.30893-02	5.30138-02	5.30138-02
^{232}Th	---	---	---	8.86989-05	8.60901-05	8.60901-05
^{234}U	---	---	---	8.88175-08	8.62051-08	8.62051-08
^{235}U	---	---	---	8.25897-06	8.01605-06	8.01605-06
^{238}U	---	---	---	5.24796-07	5.09361-07	5.09361-07
Nitrogen	2.61355-03	1.05687-05	3.92099-05	2.11606-05	2.38238-05	2.38238-05
Oxygen	---	---	1.05199-05	1.99086-04	1.93346-04	1.93346-04
Aluminum	---	---	3.80263-05	---	4.19214-07	4.19214-07

TABLE XI

Nuclide Concentrations of Spherical Unit Cell with AVR Fuel Elements of KAHTER Core B2

Nuclide	THERMOS/ISOSTO				GAM-I DIFF-2D	EXTERMINATOR-II
	Zone 1	Zone 2	Zone 3	Zone 4		
Hydrogen	2.64703-06	9.88233-06	---	6.24153-06	6.23227-06	6.23227-06
Boron	2.58204-03	7.99147-08	---	2.00767-08	2.68928-06	2.65848-06
Carbon	2.25650-02	8.42435-02	---	5.32069-02	5.31280-02	5.31280-02
^{232}Th	---	---	---	4.37929-05	4.25048-05	4.25048-05
^{234}U	---	---	---	4.74613-08	4.60653-08	4.60653-08
^{235}U	---	---	---	8.59142-06	8.33873-06	8.33873-06
^{236}U	---	---	---	2.66545-08	2.58706-08	2.58706-08
^{238}U	---	---	---	5.57776-07	5.41371-07	5.41371-07
Nitrogen	2.61355-03	1.05687-05	3.92099-05	2.11206-05	2.37850-05	2.37850-05
Oxygen	---	---	1.05199-05	3.94317-06	3.94317-06	3.94317-06
Aluminum	---	---	3.80263-05	---	4.19214-07	4.19214-07

TABLE XII

Nuclide Concentrations of Spherical Unit Cell of KAHTER Core H1

Nuclide	THERMOS/ISOSTO				GAM-I DIFF-2D	EXTERMINATOR-II
	Zone 1	Zone 2	Zone 3	Zone 4		
Hydrogen	9.98620-06	9.98620-06	---	6.24044-06	6.24069-06	6.24069-06
Boron	4.36997-05	-2.57966-08	---	2.42382-08	2.50378-07	2.19538-07
Carbon	8.51289-02	8.51289-02	---	5.31976-02	5.31997-02	5.31997-02
^{232}Th	---	---	---	8.75232-05	8.61339-05	8.61339-05
^{234}U	---	---	---	8.76401-08	8.62489-08	8.62489-08
^{235}U	---	---	---	8.14949-06	8.02013-06	8.02013-06
^{238}U	---	---	---	5.17840-07	5.09620-07	5.09620-07
Nitrogen	1.02677-05	1.02677-05	3.92099-05	2.11237-05	2.11230-05	2.11230-05
Oxygen	---	---	1.05199-05	1.96485-04	1.93429-04	1.93429-04
Aluminum	---	---	3.82401-05	---	2.26717-07	2.26717-07
^{176}Hf	1.44554-05	---	---	---	6.47772-08	6.47772-08
^{177}Hf	5.14279-05	---	---	---	2.30457-07	2.30457-07
^{178}Hf	7.54467-05	---	---	---	3.38089-07	3.38089-07
^{179}Hf	3.82260-05	---	---	---	1.71296-07	1.71296-07
^{180}Hf	9.79698-05	---	---	---	4.39018-07	4.39018-07

the assumption that the boron mass is conserved, two models were chosen:

1. Volume of the sphere is equal to the volume of the cylinder.
2. Surface of the sphere is equal to the surface of the cylinder.

The calculation with model 1 yields a k_{eff} value for core B2, which is 0.8% higher than the value of the calculation with model 2. To decide which model is adequate for the spectrum calculations, space-dependent reaction rates of $^{164}Dy(n,\gamma)^{165}Dy$ in two boron elements were measured and calculated with both models. The boron elements were irradiated in a central position of the top reflector. Reaction rate experiments in the core were not possible due to technical reasons. A comparison of measured and calculated reaction rates is given in Fig. 11.

The reaction rate decreases in the center of the element to a value of ~20%. The experiment as well as the one-dimensional ANISN (Ref. 12) calculation show a constant reaction rate outside the boron element.

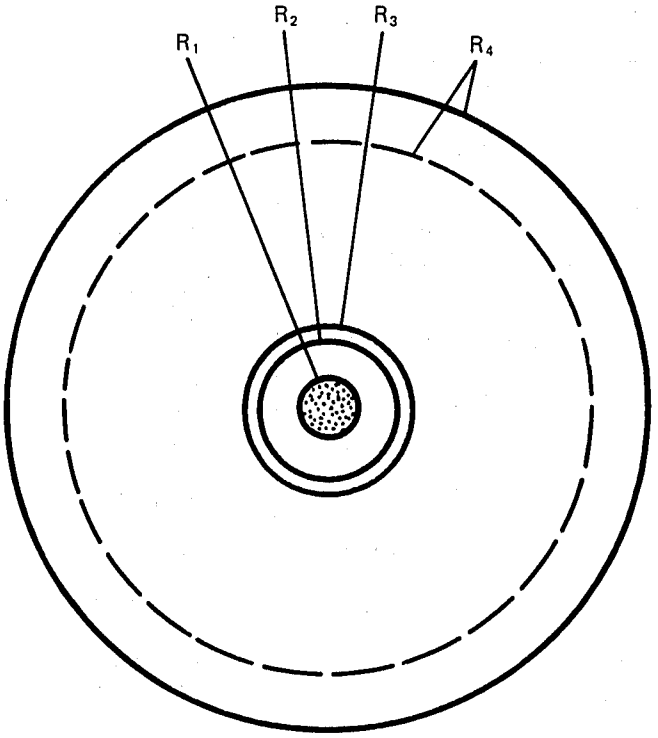

Core	R_1	R_2	R_3	R_4
B1	1.1447	3.0	3.5156	13.8392
B2	1.1447	3.0	3.5085	11.3662
H1	2.3	3.0	3.506	13.9510
H2	2.3	3.0	3.5074	12.5670
H3	2.3	3.0	3.4987	11.3344

Fig. 10. Cell model for the spectrum calculation in the KAHTER core with absorber element (dimensions in centimetres).

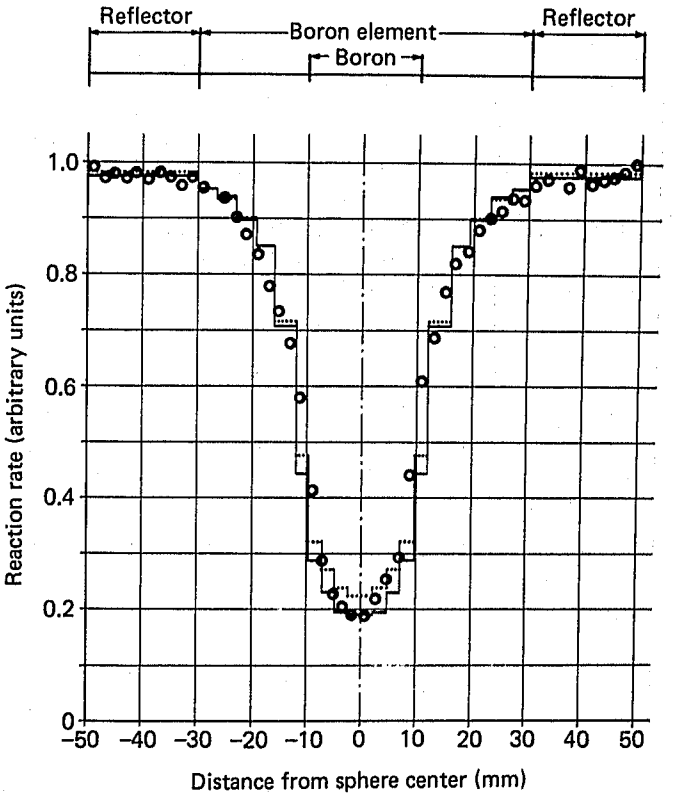

Fig. 11. Result of the measured and calculated dysprosium reaction rates in the boron absorber element.

The depression of the reaction rate inside the boron element is described better by the calculation using model 1. Therefore, model 1 was used in all further cell calculations. To determine the difference between model 1 and the real cylindrical geometry of the boron pellet, three-dimensional Monte Carlo calculations with the KENO program[13] were performed. The calculation with real geometry yields an absorption reaction rate that is 3% higher than using model 1. This is why the k_{eff} values of the B1 and B2 cores calculated with the volume equivalent cell model should be reduced by 0.15 and 0.30%, respectively. It should be mentioned here that this correction is not to be applied to the hafnium poisoned cores, because the absorption zone of the hafnium elements is of spherical geometry.

In GAMTEREX, disadvantage factor calculations are only possible in the thermal energy range using THERMOS. As the disadvantage factor of the boron pellet at 1.85-eV energy is still 0.8, disadvantage factor calculations in the epithermal and fast energy range are also necessary. These calculations must be carried out with the one-dimensional code ANISN because the spectrum code GAM-I is zero dimensional. The disadvantage factors of the boron pellet were determined over the complete energy range with ANISN. In the thermal range the factors obtained from THERMOS and ANISN are equal.

Taking into account the disadvantage factors in the epithermal and fast energy range, the k_{eff} values of the B1 and B2 cores are ~150 and 300 mNile higher, respectively. The cell model used was described in Sec. IV.D and shown in Fig. 10.

IV.F. Spectrum and Diffusion Calculations with GAMTEREX

In the calculational model, the critical facility is divided into many zones with homogenized material compositions to carry out cell and spectrum calculations with the codes GAM-I, THERMOS-Jül, and MUPO of the cycle GAMTEREX (Refs. 5 and 14). The spectra from GAM-I and THERMOS are used to produce seven-group cross sections for the two-dimensional EXTERMINATOR-2 diffusion code.[15] The energy groups are given in Table XVI.

Due to high leakage effects and the resulting strong space-dependent spectral changes in the system, a relatively fine structure in spectral zones is

TABLE XIII

Nuclide Concentrations of Spherical Unit Cell of KAHTER Core H2

Nuclide	THERMOS/ISOSTO				GAM-I DIFF-2D	EXTERMINATOR-II
	Zone 1	Zone 2	Zone 3	Zone 4		
Hydrogen	9.98620-06	9.98620-06	---	6.23361-06	6.23394-06	6.23394-06
Boron	4.36997-05	-2.57966-08	---	2.39726-08	3.21962-07	2.91155-07
Carbon	8.51289-02	8.51289-02	---	5.31393-02	5.31422-02	5.31422-02
^{232}Th	---	---	---	8.78981-05	8.59872-05	8.59872-05
^{234}U	---	---	---	8.80156-08	8.61021-08	8.61021-08
^{235}U	---	---	---	8.18440-06	8.00647-06	8.00647-06
^{238}U	---	---	---	5.20058-07	5.08752-07	5.08752-07
Nitrogen	1.02677-05	1.02677-05	3.92099-05	2.11435-05	2.11425-05	2.11425-05
Oxygen	---	---	1.05199-05	1.97317-04	1.93113-04	1.93113-04
Aluminum	---	---	3.81260-05	---	3.10157-07	3.10157-07
^{176}Hf	1.44554-05	---	---	---	8.86176-08	8.86176-08
^{177}Hf	5.14279-05	---	---	---	3.15273-07	3.15273-07
^{178}Hf	7.54467-05	---	---	---	4.62518-07	4.62518-07
^{179}Hf	3.82260-05	---	---	---	2.34340-07	2.34340-07
^{180}Hf	9.79698-05	---	---	---	6.00593-07	6.00593-07

TABLE XIV

Nuclide Concentrations of Spherical Unit Cell with THTR Fuel Elements of KAHTER Core H3

Nuclide	THERMOS/ISOSTO				GAM-I DIFF-2D	EXTERMINATOR-II
	Zone 1	Zone 2	Zone 3	Zone 4		
Hydrogen	9.98620-06	9.98620-06	---	6.28021-06	6.28066-06	6.28066-06
Boron	4.36997-05	-2.57966-08	---	2.36992-08	4.18921-07	3.87883-07
Carbon	8.51289-02	8.51289-02	---	5.35366-02	5.35405-02	5.35405-02
^{232}Th	---	---	---	8.94463-05	8.68155-05	8.68155-05
^{234}U	---	---	---	8.95658-08	8.69314-08	8.69314-08
^{235}U	---	---	---	8.32855-06	8.08359-06	8.08359-06
^{238}U	---	---	---	5.29218-07	5.13653-07	5.13653-07
Nitrogen	1.02677-05	1.02677-05	3.92099-05	2.10085-05	2.10072-05	2.10072-05
Oxygen	---	---	1.05199-05	2.00674-04	1.94887-04	1.94887-04
Aluminum	---	---	3.88933-05	---	4.22746-07	4.22746-07
^{176}Hf	1.44554-05	---	---	---	1.20786-07	1.20786-07
^{177}Hf	5.14279-05	---	---	---	4.29719-07	4.29719-07
^{178}Hf	7.54467-05	---	---	---	6.30414-07	6.30414-07
^{179}Hf	3.82260-05	---	---	---	3.19406-07	3.19406-07
^{180}Hf	9.79698-05	---	---	---	8.18611-07	8.18611-07

chosen. The homogeneity of the reflector allowed us to use the zero-dimensional spectral code MUPO. In regions of the same homogenized material compositions, spectral differences induced by neutron streaming are taken into account by the buckling and albedo recycle technique.[5,16]

In the pebble bed, the neutron streaming in the cavities between the spherical elements has to be considered in diffusion calculations. For the analysis of KAHTER experiments, the Behrens method was used. This theory had to be modified, however, to take into account statistically distributed holes.[5] The modified diffusion coefficient D_c is calculated by

$$D_c = D_h + \frac{r}{3}(1-f)\left[1+\frac{1}{8}\left(\frac{1}{1-f}\right)^2\right] ,$$

TABLE XV

Nuclide Concentrations of Spherical Unit Cell with AVR Fuel Elements of KAHTER Core H3

Nuclide	THERMOS/ISOSTO				GAM-I DIFF-2D	EXTERMINATOR-II
	Zone 1	Zone 2	Zone 3	Zone 4		
Hydrogen	9.98620-06	9.98620-06	---	6.29411-06	6.29416-06	6.29416-06
Boron	4.36997-05	-2.57966-08	---	2.02459-08	4.15636-07	3.84531-07
Carbon	8.51289-02	8.51289-02	---	5.36552-02	5.36555-02	5.36555-02
^{232}Th	---	---	---	4.41619-05	4.28630-05	4.28630-05
^{234}U	---	---	---	4.78612-08	4.64535-08	4.64535-08
^{235}U	---	---	---	8.66381-06	8.40899-06	8.40899-06
^{236}U	---	---	---	2.68791-08	2.60885-08	2.60885-08
^{238}U	---	---	---	5.62476-07	5.45932-07	5.45932-07
Nitrogen	1.02677-05	1.02677-05	3.92099-05	2.09682-05	2.09680-05	2.09680-05
Oxygen	---	---	1.05199-05	3.88775-06	3.88775-06	3.88775-06
Aluminum	---	---	3.88933-05	---	4.22746-07	4.22746-07
^{176}Hf	1.44554-05	---	---	---	1.20786-07	1.20786-07
^{177}Hf	5.14279-05	---	---	---	4.29719-07	4.29719-07
^{178}Hf	7.54467-05	---	---	---	6.30414-07	6.30414-07
^{179}Hf	3.82260-05	---	---	---	3.19406-07	3.19406-07
^{180}Hf	9.79698-05	---	---	---	8.18611-07	8.18611-07

where

D_h = diffusion coefficient of a homogeneous material

$r = 2(v_h/s)$ = hydraulic radius with v_h the void volume of a unit cell and with s the surface of one hole

f = filling factor.

The lattice structure is random and the value of r is a mean value. The effect of streaming correction has been calculated for the reference core and leads to a change of 2% in k_{eff}. The diffusion code EXTERMINATOR-2 only uses zero flux boundary condition, but the KAHTER facility has high neutron leakage. Therefore, in the calculation along boundaries, rod regions were specified to take into account an extrapolation distance. This is done in EXTERMINATOR-2 if D is input zero. The rod group constant CR is input in place of Σ_a by setting

$$CR = 1/(3 \times 0.71) = 0.469$$

for all groups.

IV.G. Spectrum and Diffusion Calculations in RSYST

The flow chart in Fig. 12 shows the module sequence used for the reactor calculations in RSYST. These calculations are performed in three steps. First, the homogenized multigroup macroscopic cross sections of the reactor zones are produced after carrying out cell calculations in spherical geometry.

TABLE XVI

Energy Boundaries for Few Group Diffusion Calculations

Group	Energy Boundaries (eV)	
	GAMTEREX	RSYST
1	$1.0 \cdot 10^{7}$	$1.4918 \cdot 10^{7}$
2	$6.393 \cdot 10^{5}$	$8.2085 \cdot 10^{5}$
3	$2.35 \cdot 10^{5}$	$9.6112 \cdot 10^{2}$
4	$1.30 \cdot 10^{2}$	$1.8554 \cdot 10^{0}$
5	$1.8554 \cdot 10^{0}$	$6.25 \cdot 10^{-1}$
6	$6.15 \cdot 10^{-1}$	$1.0 \cdot 10^{-1}$
7	$1.103 \cdot 10^{-1}$	$1.0 \cdot 10^{-5}$
	$3.9 \cdot 10^{-3}$	

Next, the few-group data are generated utilizing spectra from one-dimensional transport calculations. Finally, in a two-dimensional diffusion calculation k_{eff} of the facility and space dependent reaction rates are determined.

IV.G.1. Cell Calculations

Due to different and inhomogeneous core regions, many one-dimensional cell calculations were performed using 53-group data. Each unit cell consists

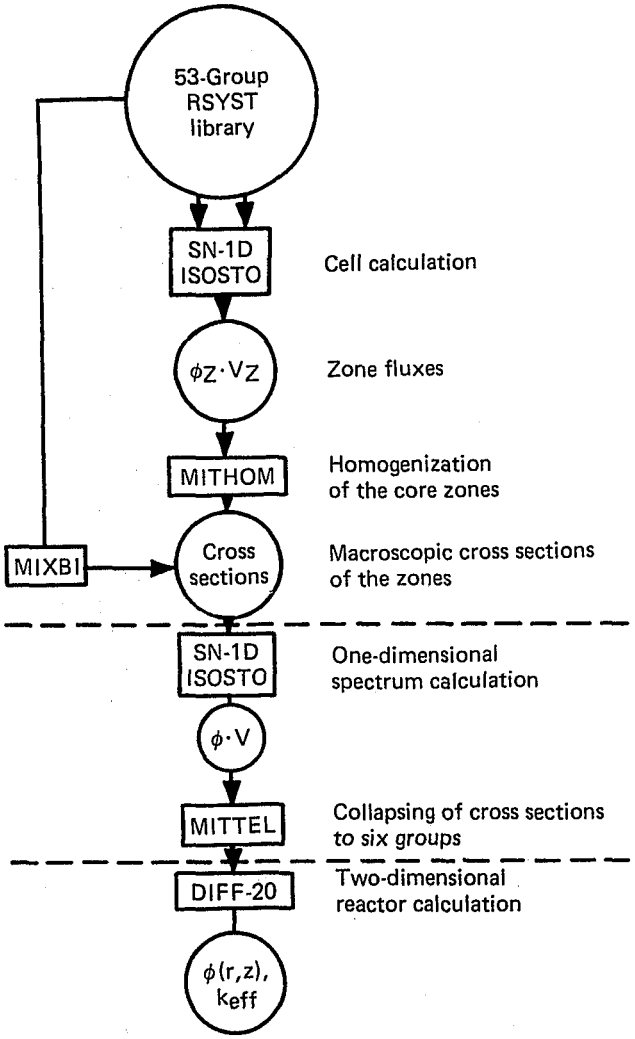

Fig. 12. Flow diagram for spectrum and diffusion calculations with RSYST.

of four zones like THERMOS cell (Figs. 10 and 11). The first two zones are identical to an absorber element and the third represents the surrounding air. The last zone of the unit cell is a homogenized shell of moderator and fuel elements and their air environment. The fuel zone containing coated particles and matrix graphite is described homogeneously taking into account the disadvantage factors of the coated particles. The cell calculations were carried out by the one-dimensional transport module SN-1D using the method of discrete ordinates in the order of S_8.

The homogenized macroscopic cross sections of the unit cell are performed by the RSYST module MITHOM utilizing the zone fluxes from the SN-1D cell calculation and the macroscopic cross sections of the four zones of the unit cell.

No cell calculations were done for the reflector. In the calculation, the channels and the graphite of the reflector regions were treated as a homogeneous mixture.

IV.G.2. Spectrum Calculations

To get few-group cross sections for the two-dimensional diffusion calculation, spectrum calculations are necessary that consider the lateral neutronic interaction between different spectral zones. These calculations are performed with the one-dimensional module SN-1D in two complementary manners, namely in axial and radial direction of the reactor.

IV.G.2.a. Axial Calculation. In the axial direction, the reactor geometry is described exactly. The necessary macroscopic cross sections are those generated by the cell calculations. The transport calculation is performed in slab geometry using the transverse buckling of the real facility.

The spectra of this calculation are used to generate few-group cross sections of the axial zones from the bottom up to the top reflector. This procedure shows that the neutronic interaction between the zones is taken into account.

IV.G.2.b. Radial Calculation. To generate the few-group cross sections of the outer core regions and the side reflector, the spectra in these regions are produced carrying out radial calculations, in which the neutronic interaction of different zones in this direction is included. In this procedure, the system is regarded as an infinitely long cylinder. This approximation is applicable to the calculation, because the nuclear property of the side reflector does not remarkably change in axial direction.

IV.G.3. Two-Dimensional Diffusion Calculation

After generating the few-group cross sections, Behrens' correction is carried out representing the streaming effect in the core and reflector cavities.

Finally, with the two-dimensional diffusion module DIFF-2D, the k_{eff} value and the flux distribution of the critical facility KAHTER are obtained. The energy group boundaries are given in Table XVI.

V. DISCUSSION OF RESULTS AND CONCLUSIONS

Comparison of experimental and theoretical results for all cores as given in Table III has been done under the same reactor conditions, i.e., without instrumentation in the bottom reflector, with a 1-mm cadmium shielding at whole surface of the facility, and with several holes in the top reflector. The measured and calculated k_{eff} values and their differences are listed in Table XVII.

For the calculations of the cores with boron absorber elements, the cylindrical boron pellet was represented by a sphere of the same volume. Investigations (Sec. IV) had shown that the real result has a value that lies between the results of the two models with the same volume and the same surface. Therefore, the results (equivalent volume model) of cores

TABLE XVII

Comparison of Experimental and Calculated k_{eff} Values

Core	Experiment k_{eff}	GAMTEREX k_{eff}	Difference GAMTEREX Experiment (%)	RSYST k_{eff}	Difference RSYST Experiment (%)
Reference	0.99681 0.99899	1.00247	0.566 0.348	0.99882	0.201 -0.017
B1	1.00389	1.00657	0.268	1.00474	0.085
B2	1.0058 0.99704 0.99949	0.99624	-0.434 -0.080 -0.325	0.99840	-0.218 0.136 -0.109
H1	1.00540	1.00841	0.301	1.00676	0.135
H2	1.00473	1.00384	-0.089	1.00355	-0.117
H3	1.00111	0.99678	-0.433	0.99973	-0.138

B1 and B2 are reduced by 0.15 and 0.30%, respectively. Table XVII shows that the core B2, which had been built up three times with the same loading and filling factor, had different experimental k_{eff} values within 0.35%. The cores with hafnium absorber elements were built up only once, but probably the experimental k_{eff} values would also vary by the same order of magnitude.

The comparison of experimental and k_{eff} values calculated with GAMTEREX shows agreement within about the range of variation of experimental k_{eff} values. Furthermore, it can be stated that, with the increasing content of absorber elements, the k_{eff} values decrease compared to the experimental results. Therefore, a certain overestimation of the absorption might occur if the portion of absorber elements has to be increased considerably.

The k_{eff} values calculated by RSYST are also listed in Table XVII. The maximum difference between experiments and calculations here is 0.218%, and therefore the calculations are in excellent agreement with the measurements.

Nuclide concentrations for both program systems were identical, and the cross sections used do not differ very much. Therefore, the differences in the results are supposed to be due to less adequate calculational models in the GAMTEREX system. The only essential difference in both program systems was in the performance of spectrum calculations. In GAMTEREX, a spectrum calculation is made for each spectral zone, and the coupling to the adjoining zones is treated only by recoupling buckling data from diffusion calculation. However, this applies only in the seven macrogroups. In RSYST, however, the spectrum calculation is performed one dimensionally through all spectral zones of the reactor in the axial or radial direction. Hence, in each calculation the spectrum influence of adjoining zones is taken into account.

Good agreement between experimental and calculational results can be stated in all cases, and so the tested models, program systems, and data bases should also give good results for larger reactor cores loaded with hafnium absorber elements.

REFERENCES

1. F. J. KRINGS, V. DRÜKE, H. JONAS, N. KIRCH, R. D. NEEF, and M. RÜCKERT, "Die Kritische Anlage KAHTER zum Hochtemperaturreaktor," Jül-1215, Kernforschungsanlage Jülich (1975).

2. H. HARDER, H. OEHME, I. SCHÖNING, and K. THURNHER, "Das 300-MW-Thorium-Hochtemperaturkernkraftwerk (THTR)," *Atomwirtschaft*, XVI, 5 (1971).

3. R. SCHULTEN, "Entstehungsgeschichte des AVR-Reaktors," *Atomwirtschaft*, 5, 218 (1966).

4. N. J. SJÖSTRAND, "Measurements on a Subcritical Reactor Using a Pulsed Neutron Source," *Arkiv För Fysik*, **11**, 233 (1956).

5. W. SCHERER, H. GERWIN, and R. D. NEEF, "Theoretische Analyse des kritischen HTR-Experimentes KAHTER," Jül-1136-RG, Kernforschungsanlage Jülich (1974).

6. R. RÜHLE, "RSYST, ein integriertes Modulsystem mit Datenbasis zur automatisierten Berechnung von Kernreaktoren," No. 4-12, Universität Stuttgart IKE-Bericht (1973).

7. R. NABI, "Entwicklung einer Rechenmethode zur HTR-Auslegung im Rahmen des Programmsystems RSYST und deren Erprobung an der kritischen Anlage KAHTER," Jül-1611, Kernforschungsanlage Jülich (1979).

8. J. KREBS, G. LE COQ, and P. RIBON, "Evaluation des Section Efficaces Neutroniques des Isotopes Stables du Hf," DPRMA-GDN, Centre d'Etude Nucleaire Saclay (Apr. 1974).

9. R. Q. WRIGHT, N. M. GREENE, I. L. LUCIUS, and C. W. CRAVEN, Jr., "SUPERTOG: A Program to Generate Fine Group Constants and Pu Scattering Matrices from ENDF/B," ORNL-TM-2679, Oak Ridge National Laboratory (1969).

10. R. BREITBARTH and E. TEUCHERT, "Resonanzintegralberechnung für mehrfach heterogene Anordnungen," Jül-551, Kernforschungsanlage Jülich (1968).

11. C. A. STEVENS and C. V. SMITH, "GAROL, A Computer Program for Evaluating Resonance Absorption Including Resonance Overlap," GA-6637, Gulf General Atomic (1965).

12. W. W. ENGLE, Jr., "A User's Manual for ANISN: A One-Dimensional Discrete Ordinates Transport Code with Anisotropic Scattering," K-1693, Oak Ridge Gaseous Diffusion Plant (1967).

13. G. E. WHITESIDES and N. F. CROSS, "KENO–A Multigroup Monte Carlo Criticality Program," CTC-5, Computing Technology Center, Oak Ridge National Laboratory (1969).

14. H. J. NEEF and W. SCHERER, "THERMOS-Jül: Modifikationen und Korrekturen am thermischen Zellprogramm THERMOS," KFA-IRE-IB-26/72, Kernforschungsanlage Jülich Institut für Reaktorentwicklung (1972).

15. T. B. FOWLER, M. L. TOBIAS, and D. R. VONDY, "EXTERMINATOR-2: A Fortran IV Code for Solving Multigroup Neutron Diffusion Equations in Two Dimensions," ORNL-4078, Oak Ridge National Laboratory (1967).

16. W. FRÖHLING, "Beiträge zur Neutronenphysik des Kugelhaufenreaktors," Jül-771-RG, Kernforschungsanlage Jülich (1971).